Propagation of surface waves over an imperfectly coated half-space with a Winkler-Fuss loading

Maha M. Helmi

Department of Mathematics and Statistics, College of Science, Taif University, P.O. Box 11099, Taif 21944, Saudi Arabia.
Email: m.hlmi@tu.edu.sa

Abstract

In this study, we demonstrate how elastic surface waves propagate on a coated cylindrical half-space. The coated structure is assumed to have generalized imperfect conditions on the interface that binds the coating and half-space layers, while at the same time, it is endowed with a Winkler-Fuss elastic foundation through the coating medium, serving as a shearing mechanical loading. Through the application of both the classical and approximation methods, the consequential dispersion relation has been acquired, in addition to the acquisition of the overall vibrational displacements in the respective layers. In particular, an approximate equation of anti-plane motion through the application of the asymptotic approximation method has been acquired while doing away with the interfacial imperfection; the untapped asymptotic approximation techniques that derive the related effective boundary conditions have been deployed. Moreover, some realistic contrast setups have been analyzed in the end, showing the significance of all the imposed effects on the dispersion of waves in the coated medium. Comparatively, the derived approximate results have been noted to agree with the corresponding analytical results. Additionally, the derived approximate expressions for the phase and group velocities have been examined, which showed the significance of mechanical loading and the shear speed ratio on the propagating shear waves in the coated medium.
Keywords: Anti-plane shear motion, coated half-space, cylindrical composites, imperfect interface, elastic foundations, asymptotic analysis.

1 Introduction

Propagation of surface waves on elastic structures and composites is an important phenomenon of contemporary interest. The recent development in modern structures and materials has triggered vast interest from the research community to propose optimal models and methods for perfect implementation and analysis, respectively [1, 2, 3]. Mathematically, various researchers have both recently and long ago modeled the propagation of surface waves in composite and multilayered media; like modeling the vibration of waves in compressible pre-stressed plates ï¿œ[4], asymptotic techniques for handling effects of external forces on a vibrating coated halspace [5], method for examining coated multi-layered semi-infinite body [6], and the nondestructive method for Love wave analysis among others [7]. More so, other aspects of interest include the the interaction waves with other effects in multilayered media, which are mainly imposed effects like thermal stresses, rotational frames, and gravitational fields [8, 9], and mechanical loads [10, 11], ï¿œthat are exerted externally, and the on the other hand, the vast relevance of sliding contact conditions presumed on the interfaces of the multilayered structures, the so-called imperfect interfacial conditions [12, 13]. Certainly, these two phenomena of elastic foundations and imperfect interface between layers have been extensively examined in relation to elastic structures that appear mostly in rectangular coordinate systems, with a few studies concerning structures in cylindrical and spherical coordinate settings. In addition, the importance of elastic foundations in supporting the geometrical configuration of elastic structures can never be overemphasized. For this season, the literature is full of various considerations and proposals for elastic foundations, with the view to attaining perfect structural dynamics. In particular, we make mention of the Pasternak and Hetenyi elastic foundations [14], and the variable-dependent inhomogeneous elastic foundations [15], which account for material inhomogeneities in the supported foundation; read also the recently devised foundations, that feature viscoelastic property in nonlinear and functionally graded media (FGM), correspondingly in [16] and [17]. Moreover, the mention of viscoelastic property has led to briefly discussing some of the breakthroughs of our recent times, where various viscoelastic structures have been proposed, and further actualized with vast applications in modern sciences. Indeed, diverse scientists have examined the wave movement in viscoelastic media and materials, including multi-layered structures. For instance, Kumari et al. [18] discussed the relevance of Love waves on a corrugated orthotropic damped visco-elastic FGM plate, while Saha et al [19] examined the pattern of shear waves on multilayered fiber-reinforced viscoelastic composite. In the same vein, Kundu and Kumari [20] examined to wave dynamics of a torsionally propagating inhomogeneous crustal overlying a viscoelastic half-space using analytical approach, while ï¿œAbd-Alla et al. [21] infused the effects of rotation, magnetic and thermal fields on reinforced viscoelastic anisotropic medium through the application of a classical method; see also the lately submission by Elmoghazy et al. [22] that deployed effective numerical process to modeling and analysis the significance f damping and viscoelasticity on vibrating composite bodies.

However, motivated by the lack of sufficient study in cylindrical systems that deeply examine the wave dynamics in multilayered structures, the present study thus aimed at unraveling the necessary know-how on how elastic surface waves propagate on a coated cylindrical half-space. The coated medium will be based on the assumption that the interface between the coating and the half-space layer is sliding, in addition to the excitation of the Winkler-Fuss mechanical loading via the coating surface. Moreover, with the help of both the analytical and asymptotic methods, the consequential vibrational displacements, stresses, and the dispersion relation will be acquired and further examined to assess the most significant wave parameters. In particular, the study will attempt to derive the approximate equation of motion for the propagation of anti-plane shear waves in the perfectly coated half-space using the asymptotic approximation method [5] - indeed, an approach that superbly works on perfectly welded mediums in a general sense; the case of imperfectly welded mediums remains open for generalization. Additionally, some realistic contrast setups of coated half-spaces will be considered for numerical study, while a comparative study will be established for the approximate and exact dispersion relations to be unraveled. What is more, as the approximate dispersion relation gives room for in-depth analysis, the related approximate expressions for the phase and group velocities will be analyzed to equally assess the wave dynamics in governing the coated body. Moreover, this study will apply to a variety of fields, like the material and geophysical sciences, among others, where, despite the huge literature, scientists still explore avenues for the description of intricate scenarios. As a particular case, scientists are curious to find out the salient properties of the Earth's interior concerning its heterogeneous nature in terms of the density and characteristics [23]. In addition, the effect of initially pre-stresses and nonlinear foundation supports are still of interest in the construction of mini and gigantic structures [24], including the effect of thermal stresses in thermoelastic structures [25, 26], the interaction of fluids with nano-particles [27], and lastly the influence of damping force on the dispersion of surface waves in coated medium [28], among others.

Finally, this manuscript is arranged as follows: Section 2 gives the formulation of the model to be studied. Section 3 states the related imposed boundary and interfacial data. Section 4 derived the exact analytical wave fields. Section 5 derives the exact expression for the dispersion relation. Section 6 presents the numerical results. Section 7 derives an approximate model for a perfect contact interface, while Section 8 provides the concluding remarks.

2 Problem formulation

This study considers the anti-plane shear motion in a cylindrical coordinate system [29], where the displacement fields take the following setting: $u_r = 0$, $u_\theta = u(r, z, t)$ and $u_z = 0$, where r is the radius of the cylinder, z is the azimuthal variable, while t is the temporal variable. Further, with the consideration of a coated cylindrical half-space - see Figure 1 - the equations of anti-plane shear motion in the respective layers are presided over by the following out-of-plane equations

$$\frac{\partial \tau_{r\theta}^{p}}{\partial r} + \frac{\partial \tau_{\theta z}^{p}}{\partial z} + \frac{2}{r}\tau_{r\theta}^{p} = \rho_p \frac{\partial^2 u_p}{\partial t^2}, \qquad p = 1, 2, \tag{1}$$

where u_p are the out-of-plane displacement fields in the coating ($0 \le z \le h$) when $p = 1$, and the half-space ($h \le z < \infty$) when $p = 2$; h is a finite thickness.

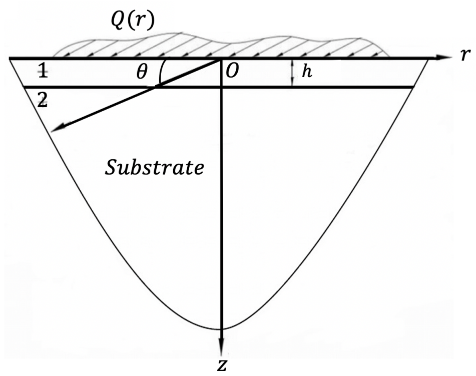

Figure 1: Geometry of the cylindrical problem.

In addition, $\tau_{r\theta}$ and $\tau_{\theta z}^{p}$ are the related shear stresses expressed as follows [20]

$$\tau_{r\theta}^{p} = \mu_p \left(\frac{\partial u_p}{\partial r} - \frac{u_p}{r} \right), \qquad \text{and} \qquad \tau_{\theta z}^{p} = \mu_p \frac{\partial u_p}{\partial z}, \qquad p = 1, 2, \tag{2}$$

where μ_p for $p = 1, 2$ are the material constants in the layers of the coated cylinder, while ρ_p are the corresponding densities in the layers. Besides, it is pertinent to mention here that mentioned shear stresses in Eq. (2) are plainly the non-vanishing anti-plane stresses that satisfy the out-of-plane displacement field $u_\theta = u(r, z, t)$; for more on the complete normal and shear stress fields, one is referred to [20].

3 Boundary and interfacial conditions

Boundary condition. The related boundary condition at surface of the structure, that is, at $z = 0$, is considered to be a mechanical load as follows P as follows

$$\tau_{\theta z}^{1} = -Q, \quad \text{at} \quad z = 0, \tag{3}$$

Certainly, upon considering the mechanical load to be due to the Winkler-Fuss elastic foundation, Q then takes the following expression [9]

$$Q = \chi u_1, \tag{4}$$

where χ is the rigidity of the Winkler-Fuss elastic foundation. Moreover, when $\chi = 0$, the loading reduces to that of the known case of traction-free surface, where Eq. (3) thus becomes the following condition

$$\tau^1_{\theta z} = 0, \quad \text{at} \quad z = 0. \tag{5}$$

Furthermore, with regards to the boundary condition along the depth of the coated cylindrical structures, a natural condition is imposed as $z \to \infty$ as follows

$$u_2 \to 0, \quad \text{as} \quad z \to \infty, \tag{6}$$

ensuring a bounded vibrational displacement u_2 as the thickness of the half-space layer stretches to infinity.

Interfacial conditions. Concerning the interfacial conditions to be imposed on the interface of the cylindrical coating and the half-space, the following physical options will be examined:

(a) Perfect interface. Perfect contact conditions are achieved on the governing interface of the two-layered structure on attaining perfection by the related vibrational displacements and stresses on the interface. In particular, given the interface of the present coated half-space to be at $z = h$, the prescribed perfect contact conditions thus take the following forms

$$\begin{aligned} u_1 - u_2 &= 0, & \text{at} \quad z &= h, \\ \tau^1_{\theta z} - \tau^2_{\theta z} &= 0, & \text{at} \quad z &= h. \end{aligned} \tag{7}$$

(b) Imperfect interface. Since interfaces are frown to sliding by the gradual de-lamination process that is caused by several physical phenomena, the present structure is equally assumed to undergo a sliding process at the interface, $z = h$ upon prescribing the following generalized sliding contact conditions [13]

$$\begin{aligned} u_1 - u_2 &= \psi \tau^2_{\theta z}, & \text{at} \quad z &= h, \\ \tau^1_{\theta z} - \tau^2_{\theta z} &= 0, & \text{at} \quad z &= h, \end{aligned} \tag{8}$$

where $\psi \neq 0$ is the imperfect interface (sliding contact) parameter; besides, one gets the perfect interface earlier expressed in Eq. (7) when $\psi = 0$. In addition, some recent studies suggest generalized interfacial conditions, which may include a corrugated interface due to various physical reasons, read [30, 31] and the references therein for more on generalized interfaces.

4 Exact wave fields

To solve the governing model for the propagation of waves in solid medium, one first re-writes Eq. (1) using the constitutive relations in Eq. (2) as follows

$$\frac{\partial^2 u_p}{\partial r^2} + \frac{1}{r}\frac{\partial u_p}{\partial r} - \frac{u_p}{r^2} + \frac{\partial^2 u_p}{\partial z^2} = \frac{1}{c_p^2}\frac{\partial^2 u_p}{\partial t^2}, \qquad p = 1, 2, \tag{9}$$

where c_p for $p = 1, 2$, are expressed as follows

$$c_p = \sqrt{\frac{\mu_p}{\rho_p}}, \qquad p = 1, 2, \tag{10}$$

which are the shear speeds in the respective cylindrical layers.

Next, Eq. (9) features the Bessel differential equation of order one in the radial variable r, therefore, a harmonic wave solution is considered to solve the equation as follows [32]

$$\begin{aligned} u_1(r, z, t) &= V_1(z)J_1(kr)e^{i\omega t}, \\ u_2(r, z, t) &= V_2(z)J_1(kr)e^{i\omega t}, \end{aligned} \tag{11}$$

where k is the dimensional wavenumber, $J_1(.)$ is the Bessel function of the first kind of order one, ω is the angular frequency, i is the imaginary unit, while $V_p(z)$ for $p = 1, 2$ are the respective amplitudes in the radial direction z.

Accordingly, upon utilizing Eq. (11) into Eq. (9), the following reduced simple linear differential equations are thus obtained

$$\frac{d^2 V_p}{dz^2} - \alpha_p^2 V_p \quad = 0, \qquad p = 1, 2, \tag{12}$$

where α_p in the latter equation are expressed as follows

$$\alpha_p = \sqrt{k^2 - \frac{\omega^2}{c_p^2}}, \qquad p = 1, 2. \tag{13}$$

Further, one gets the exact solutions for Eq. (12) in the respective layers of the coated structures as follows

$$\begin{aligned} V_1(z) =& A_1 \cosh(\alpha_1 z) + B_1 \sinh(\alpha_1 z), \quad 0 \le z \le h, \\ V_2(z) =& A_2 e^{-\alpha_2 z} + B_2 e^{\alpha_2 z}, \qquad\qquad h \le z < \infty, \end{aligned} \tag{14}$$

where A_1, B_1, A_2, and B_2 are constants to be determined shortly from the imposed boundary and interfacial data.

In the same vein, one gets the respective displacement fields in the governing layers of the coated body from Eq. (11) and (14) as follows

$$
\begin{aligned}
u_1(r,z,t) =& (A_1 \cosh(\alpha_1 z) + B_1 \sinh(\alpha_1 z)) J_1(kr) e^{i\omega t}, && 0 \le z \le h, \\
u_2(r,z,t) =& A_2 J_1(kr) e^{-\alpha_2 z + i\omega t}, && h \le z < \infty,
\end{aligned}
\tag{15}
$$

where A_1, B_1 and A_2 are to be determined, while $B_2 \to 0$ as $z \to \infty$, that is, for an ensured bounded solution at infinity.

5 Exact dispersion relation

First, let us begin the section by introducing the following non-dimensionalization

$$
\mu = \frac{\mu_1}{\mu_2}, \qquad \rho = \frac{\rho_1}{\rho_2}, \qquad \mho = \frac{c_1}{c_2}, \tag{16}
$$

where μ rigidity ratio, ρ density ratio, and $\mho$ is the shear speed ratio; the respective shear speeds in the coating and half-space layers are already expressed in Eq. (10).

Accordingly, with the utilization of the imposed boundary and interfacial conditions in Eqs. (3)-(8), one obtains the following dispersion matrix, which subsequently yields the resultant exact dispersion relation. Moreover, in what follows, we make considerations of the perfect and imperfect interfacial cases.

A coated cylindrical half-space with a perfect interface

Here, with the consideration of a perfect interface between the two layers in the presence of a mechanical loading earlier expresses in Eqs. (3)-(6) and (7), the resulting dispersion matrix in the present setting can be expressed as follows

$$
A_1 = \begin{pmatrix} X & \xi_1 & 0 \\ \cosh(\xi_1) & \sinh(\xi_1) & -e^{-\xi_2} \\ \sinh(\xi_1) & \cosh(\xi_1) & \frac{e^{-\xi_2}\xi_2}{\mu\xi_1} \end{pmatrix}, \tag{17}
$$

where

$$
\xi_1 = \sqrt{K^2 - \Omega^2}, \qquad \xi_2 = \sqrt{K^2 - \mho^2\Omega^2}, \tag{18}
$$

with K, Ω and X denoting the dimensionless wave number, angular frequency and the dimensionless stiffness of the mechanical load, respectively expressed as follows

$$
K = kh, \qquad \Omega = \frac{\omega h}{c_1}, \qquad X = \frac{\chi h}{\mu_1}. \tag{19}
$$

Accordingly, with the determination of the dispersion matrix in Eq. (17), being the coefficient matrix of the resulting homogeneous equation acquired from the imposed boundary and interfacial conditions, the consequent dispersion relation is therefore obtained after setting the determinant of the said matrix to zero as follows

$$\left(\xi_2 X - \mu\xi_1^2\right)\sinh\left(\xi_1\right) - \xi_1\left(\xi_2 - \mu X\right)\cosh\left(\xi_1\right) = 0, \tag{20}$$

or alternatively upon dividing the latter equation with $\cosh\left(\xi_1\right)$ the following reduced dispersion relation

$$\left(\xi_2 X - \mu\xi_1^2\right)\tanh\left(\xi_1\right) = \xi_1\left(\xi_2 - \mu X\right). \tag{21}$$

Notably, the realization and satisfaction of the exact dispersion relation in Eq. (21) insures the formulated model to admits non-trivial displacement fields u_p for $p = 1, 2$ in the respective layers of the medium.

Moreover, in the absence of the acting mechanical load on the surface of the coated body, the dimensionless stiffness of the mechanical load vanishes, that is, $X = 0$, which further reduces the dispersion relation in Eq. (21) to the following

$$\mu\xi_1\tanh\left(\xi_1\right) = -\xi_2. \tag{22}$$

A coated cylindrical half-space with an imperfect interface

With the consideration of an imperfect interface between the coating and the half-space layers, the imposed boundary conditions (3)-(6) and the sliding contact condition (8) results in the following dispersion matrix

$$A_2 = \begin{pmatrix} X & \xi_1 & 0 \\ \cosh\left(\xi_1\right) & \sinh\left(\xi_1\right) & e^{-\xi_2}\left(\Psi\xi_2 - 1\right) \\ \sinh\left(\xi_1\right) & \cosh\left(\xi_1\right) & \frac{e^{-\xi_2}\xi_2}{\mu\xi_1} \end{pmatrix} \tag{23}$$

where ξ_1, ξ_2 and X are dimensionless quantities already expressed in Eq. (18)-(19), while Ψ is the dimensionless imperfect contact parameter, the parameter responsible for sliding interface, expressed as follows

$$\Psi = \frac{\psi\mu_2}{h}. \tag{24}$$

In addition, with the acquisition of the dispersion matrix in Eq. (23), the subsequent exact dimensionless dispersion relation is thus obtained upon equating the resulting determinant of the matrix to zero as follows

$$\left(\mu\left(\xi_2\Psi - 1\right)\xi_1^2 + \xi_2 X\right)\tanh\left(\xi_1\right) = \xi_1\left(\left(\mu X\Psi + 1\right)\xi_2 - \mu X\right). \tag{25}$$

In particular, the absence of the imperfect interface, that is, when the interface between the two layers is perfectly bonded, one sets $\Psi = 0$ in the above equation to obtain the stated dispersion relation in Eq. (21); equally, the absence of both the perfect contact and mechanical load reduces the latter dispersion relation to the reduced dispersion relation in Eq. (22). In addition, amidst the presence of sliding contact on the interface with free surface, the mechanical load, in the form of the Winkler-Fuss foundation, is thus disregarded, leading to setting $X = 0$ in the latter dispersion equation to obtain yet a reduced equation as follows

$$\mu\xi_1\left(\xi_2\Psi - 1\right)\tanh\left(\xi_1\right) = \xi_2. \tag{26}$$

Besides, one gets the reduced dispersion relation in Eq. (22) from Eq. (26) upon setting $\Psi = 0$, which corresponds to the dispersion relation for a perfectly coated half-space that is exposed to free-surface.

6 Numerical results

This section numerically examines the derived exact dispersion relation in ï¿œEq. (25) that governs the propagation of shear waves on a coated cylindrical half-space with imperfect interface and the action of Winkler-Fuss mechanical load. Thus, considering the coating layer to be made of aluminium material, while the half-space is made of zinc material; see Tabel 1 for the physical data of these materials, where the Lame's constants μ_p for $p = 1, 2$ are related to the Poisson ratio ν_p and the Young's modull E_p through $\mu_p = \frac{E_p}{2(1+\nu_p)}$ for $p = 1, 2$. Furthermore, Figures 2, 3, and 4 examine the significance of varying the sliding contact paramater (imperfect contact paramater) X, the ï¿œWinkler-Fuss paramaeter foundation Ψ, and the variation of the shear speed ratio $\mho$, respectively on the phase speed versus wave number K plot. ï¿œ Accordingly, from Figure 2, it is noted that an increase in the sliding contact parameter Ψ increases the dispersion of waves in the coated medium, with the perfect contact situation portraying the least dispersion, that is, when $\Psi = 0$. ï¿œMoreover, as the plot has been based upon a stiff foundation, that is, when $X = 0.8$, it is concluded that the presence of interfacial imperfection increases the dispersion of waves in the medium. ï¿œ

In addition, Figure 3 examines the significance of the action of the mechanical load X on the evolution of waves in the coated medium, the so-called Winkler-Fuss elastic foundation. Notably, one notes that an increase in Winkler-Fuss elastic foundation parameter X decreases the dispersion of waves in the medium; moreover, a kind of stiff elastic foundation values have been used ($X = 0.75, 0.80, 0.85$) for more visibility. However, this is physically realistic as the coated medium is mechanically loaded, which suppresses the vibration in the medium. ï¿œ

Lastly, Figure 4 assesses the impact of the shear speed ratio $\mho$ on the dispersion of waves in the medium. Indeed, with the consideration of the coating, and the half-space layers to be of aluminum and zinc material, respectively, $\mho = \frac{c_1}{c_2}$ has been found to be $\mho \approx 0.267559$. Thus, Figure 4 captures the dispersion trend when the shear speed ratio $\mho$ assumes $0.267559, 0.367559$, and 0.467559. Consequently, one notes from these curves that maximum rise has been associated with the benchmark shear speed ratio of aluminum/zinc, while increasing the speed ratio decreases the dispersion in the medium.

Table 1: Most related literature [5, 33].

Layer, (p)	Material	E_p $(\times 10^{10})$ Nm^{-2}	ν_p	ρ_p $(\times 10^3)$ kgm^{-3}
Coating, $(p = 1)$	Aluminium	2.7	0.31	2.643
Half-space, $(p = 2)$	Zinc	96.6	0.249	7.1

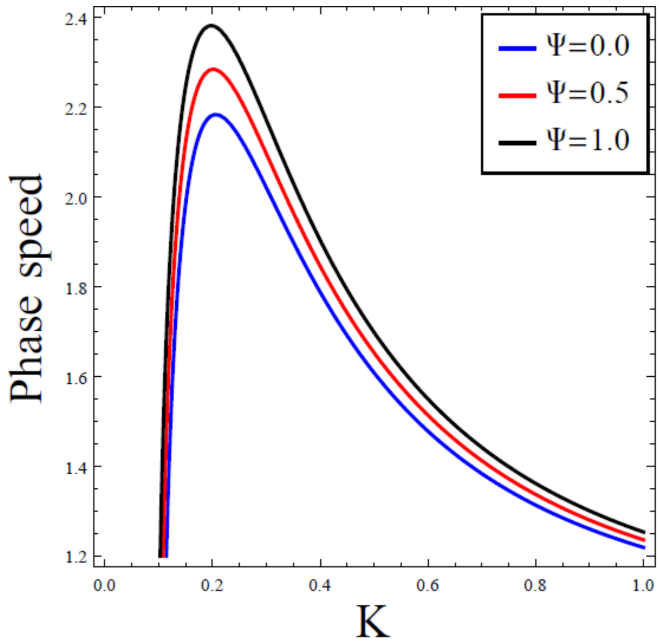

Figure 2: Significance of sliding contact parameter Ψ on the dispersion of waves in the coated medium when $X = 0.8$.

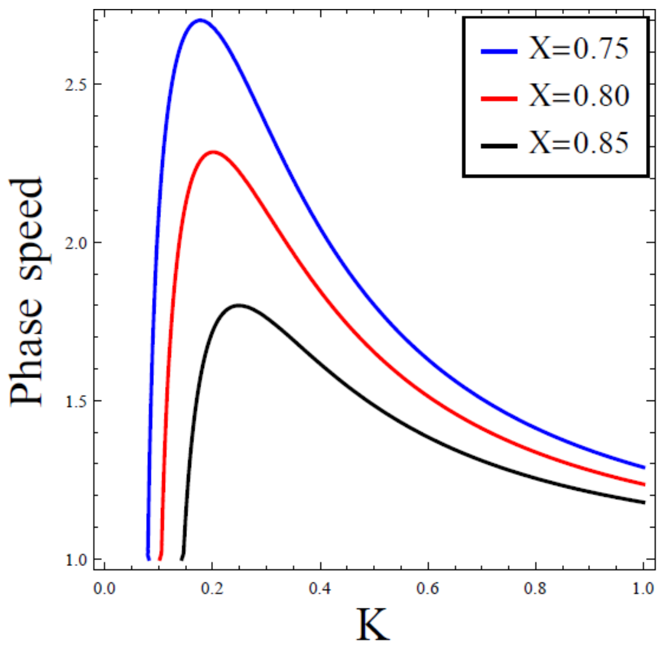

Figure 3: Significance of Winkler-Fuss foundation parameter X on the dispersion of waves in the coated medium when $\Psi = 0.5$.

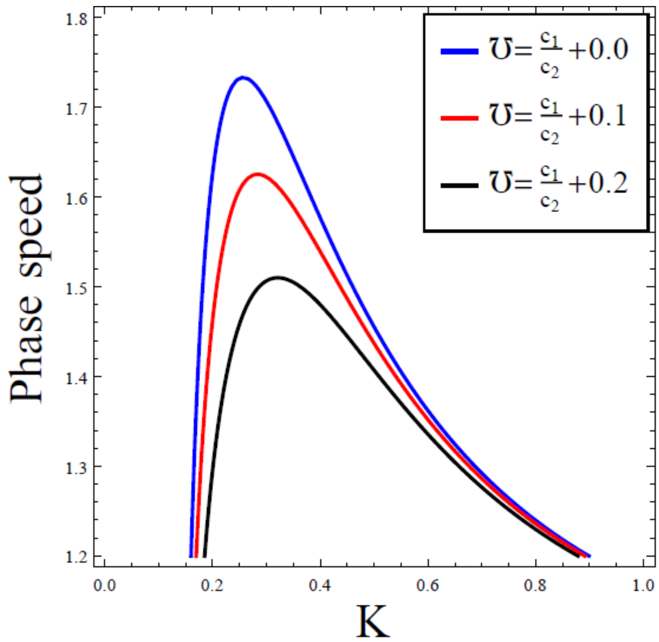

Figure 4: Significance of shear speed ratio $\mho$ on the dispersion of waves in the coated medium when $X = 0.85$ and $\Psi = 0.2$.

7 Approximate model for perfect contact

Since it is a known fact approximate model for the propagation of waves in multi-layered mediums exists only for perfectly bonded multi-layered composites, this section then utilizes the asymptotic approximation approach [5, 6] to derive the approximate model for perfect interfacial contact. Thus, the section begins with the derivation of the model's effective boundary conditions using the procedure outlined in [34, 35].

Therefore, to begin with, let us consider the thickness of the coating layer h to be very small compared to a typical length scale L that is related to the long wave region; mathematically, we write

$$\varepsilon = \frac{h}{L} \ll 1. \tag{27}$$

Next, we yet consider the imposed boundary condition on the surface $z = h$, to be

$$u_2 = v, \tag{28}$$

where $v = v(r, t)$ is displacement on the interfacial surface of the substrate.

Additionally, let us introduce the following scaling variables

$$R = \frac{r}{L}, \qquad \eta = \frac{z}{h}, \qquad \text{and} \qquad \tau = \frac{t\, c_1}{L}, \tag{29}$$

coupled with the following dimensionless quantities

$$u_1^* = \frac{u_1}{L}, \qquad v^* = \frac{v}{L}, \qquad \chi^* = \frac{\chi\, h}{\varepsilon^2\, \mu_1}. \tag{30}$$

Thus, the governing equation of motion provided in Eq. (9), and the boundary conditions in Eqs. (3) and (28) can be rewritten in terms of the latter new dimensionless quantities as follows

$$\frac{\partial^2 u_1^*}{\partial \eta^2} + \varepsilon^2 \left(\frac{\partial^2 u_1^*}{\partial R^2} + \frac{1}{R}\frac{\partial u_1^*}{\partial R} - \frac{u_1^*}{R^2} - \frac{\partial^2 u_1^*}{\partial \tau^2} \right) = 0, \tag{31}$$

subject to the following transformed boundary conditions

$$\begin{aligned} \frac{\partial u_1^*}{\partial \eta} &= -\varepsilon^2\, \chi^*\, u_1^*, \quad &&\text{at} \quad \eta = 0, \\ u_1^* &= v^*, &&\text{at} \quad \eta = 1. \end{aligned} \tag{32}$$

Accordingly, expanding the involving displacements u_p^* for $p = 1, 2$, and the stress $\tau_{\theta z}^*$ as follows

$$u_p^* = u_p^{(0)} + \varepsilon^2\, u_p^{(2)} + ... \tag{33}$$

and

$$\tau_{\theta z}^* = \frac{\partial}{\partial \eta} \left(u_p^{(0)} + \varepsilon^2\, u_p^{(2)} + ... \right), \tag{34}$$

where $\tau_{\theta z}^*$ is the dimensionless stress, explicitly expressed as follows

$$\tau_{\theta z}^* = \frac{\varepsilon\, \tau_{\theta z}^1}{\mu_1}.$$

Next, substituting the asymptotic expansions in Eqs. (33) and (34) into Eqs. (31) and (32), one gets at leading order $O(1)$ the following reduced equation

$$\frac{\partial^2 u_1^{(0)}}{\partial \eta^2} = 0, \tag{35}$$

subject to the following boundary data

$$\begin{aligned} \frac{\partial u_1^{(0)}}{\partial \eta} &= 0, \quad &&\text{at} \quad \eta = 0, \\ u_1^{(0)} &= v^{(0)} &&\text{at} \quad \eta = 1. \end{aligned} \tag{36}$$

Hence, from the latter boundary-value problem in Eqs. (35)-(36), one deduces that

$$u_1^{(0)} = v^*, \tag{37}$$

which necessitates further analysis. Next at next order, that is, $O\left(\varepsilon^2\right)$, one equally substitutes the asymptotic expansions in Eqs. (33) and (34) into Eqs. (31) and (32), and gets the boundary-value problem at the order $O\left(\varepsilon^2\right)$ as follows

$$\frac{\partial^2 u_1^{(2)}}{\partial \eta^2}+\left(\frac{\partial^2 u_1^{(0)}}{\partial R^2}+\frac{1}{R}\frac{\partial u_1^{(0)}}{\partial R}-\frac{u_1^{(0)}}{R^2}-\frac{\partial^2 u_1^{(0)}}{\partial \tau^2}\right)=0, \tag{38}$$

subject to the following boundary conditions

$$\begin{aligned} \frac{\partial u_1^{(2)}}{\partial \eta} &= -\chi^*\, u_1^{(0)}, \quad \text{at} \quad \eta=0,\\ u_1^{(2)} &= 0, \qquad\qquad \text{at} \quad \eta=1. \end{aligned} \tag{39}$$

Consequently, having determined $u_1^{(0)}=v^*$ from Eq. (37), the solution of Eq. (38) satisfying the imposing conditions in Eq. (39) is found as follows

$$u_1^{(2)}=\frac{1}{2}\left(1-\eta^2\right)\left(\frac{\partial^2 v^*}{\partial R^2}+\frac{1}{R}\frac{\partial v^*}{\partial R}-\frac{v^*}{R^2}-\frac{\partial^2 v^*}{\partial \tau^2}\right)+(1-\eta)\,\chi^*\,v^*, \tag{40}$$

which equally yields the involving stress field from Eq. (34) as follows

$$\tau_{\theta z}^{*}=\varepsilon^2\left(-\eta\left(\frac{\partial^2 v^*}{\partial R^2}+\frac{1}{R}\frac{\partial v^*}{\partial R}-\frac{v^*}{R^2}-\frac{\partial^2 v^*}{\partial \tau^2}\right)-\chi^*\,v^*\right)+O\left(\varepsilon^2\right). \tag{41}$$

Furthermore, re-writing the later stress function in terms of the original dimensional variables, one thus gets

$$\tau_{\theta z}^{1}=z\left(\rho_1\frac{\partial^2 v}{\partial t^2}-\mu_1\left(\frac{\partial^2 v}{\partial r^2}+\frac{1}{r}\frac{\partial v}{\partial r}-\frac{v}{r^2}\right)\right)-\chi\, v. \tag{42}$$

Accordingly, the superimposed perfect contact conditions, that is, the continuity of stress and displacement at the interface, $z=h$ give in the following effective boundary conditions

$$\tau_{\theta z}^{2}=h\left(\rho_1\frac{\partial^2 u_2}{\partial t^2}-\mu_1\left(\frac{\partial^2 u_2}{\partial r^2}+\frac{1}{r}\frac{\partial u_2}{\partial r}-\frac{u_2}{r^2}\right)\right)-\chi\, u_2. \tag{43}$$

Moreover, the approximate model for the propagation of shear waves on a perfectly coated half-spaces is obtained by inserting Eq. $(2)_2$ and the solution expressed in Eq. $(15)_2$ into Eq. (43) as follows

$$h\left(\rho_1\frac{\partial^2 u_2}{\partial t^2}-\mu_1\left(\frac{\partial^2 u_2}{\partial r^2}+\frac{1}{r}\frac{\partial u_2}{\partial r}-\frac{u_2}{r^2}\right)\right)-\chi\, u_2-\mu_2\frac{\partial u_2}{\partial z}=0. \tag{44}$$

Lastly, one obtains the consequential approximate dispersion relation from the just derived approximate equation of motion in Eq. (44) upon inserting the earlier considered harmonic solution in Eq. $(11)_2$, that is, $u_2(r,z,t)=A_2J_1(kr)e^{-\alpha_2 z+i\omega t}$, as follows

$$\chi-\alpha_2\mu_2-hk^2\mu_1+h\rho_1\omega^2=0, \tag{45}$$

or equally upon non-dimensionalizing the following expression approximate dispersion result

$$X-\frac{\xi_2}{\mu}-K^2+\Omega^2=0, \tag{46}$$

where ξ_2 is in Eq. (18) as $\xi_2 = \sqrt{K^2 - \mho^2\Omega^2}$. In particular, Figure 5 gives the comparison between the exact dispersion relation Eq. (21) and the approximate dispersion relation Eq. (46) - through their respective fundamental modes - where a significant agreement has been noted between the two curves.

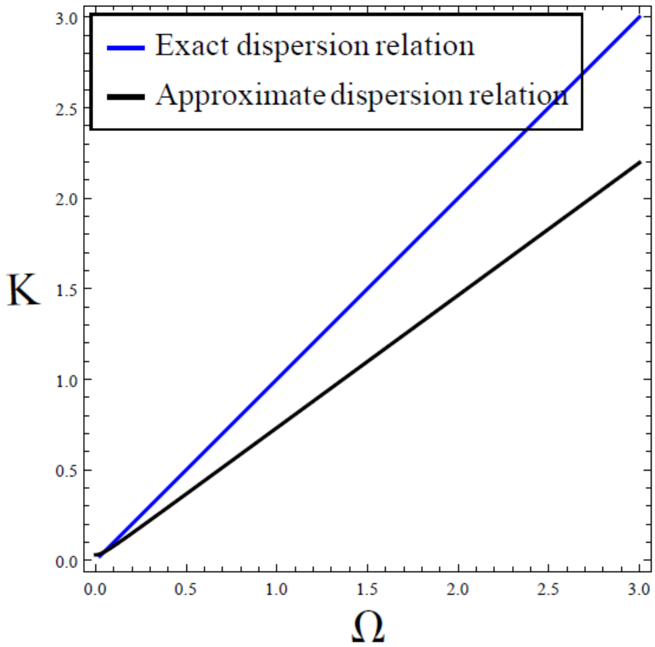

Figure 5: Comparison of the exact Eq. (21) and approximate Eq. (46) dispersion relations - through fundamental mode curves when $X = 0.002$.

Thus, with the acquisition of the approximate dispersion relation in Eq. (46), one can proceed with various wave analyses, including the analysis of the related phase and group velocities, which is not that straightforward using the exact expression for the dispersion relation. In this regard, considering the positive values, one obtains the approximate consequential phase and group velocities, respectively, from Eq. (46) as follows

$$\begin{aligned}\text{Phase velocity} &= \frac{\Omega}{K} \approx \frac{\sqrt{2}\Omega}{\sqrt{X + \Omega^2(\mho^2+1)}},\\ \text{Grough velocity} &= \frac{\mathrm{d}\Omega}{\mathrm{d}K} \approx \frac{\sqrt{2}\sqrt{X + \Omega^2\left(\mho^2+1\right)}}{\Omega\left(\mho^2+1\right)}.\end{aligned} \tag{47}$$

Moreover, one notes from the above approximate velocities that the absence of the Winkler-Fuss load on the coated cylinder leads to $X = 0$, which necessitates the velocities to become equal as follows

$$\text{Phase velocity} = \text{Grough velocity} \approx \frac{\sqrt{2}}{\sqrt{\mho^2+1}}. \tag{48}$$

In addition, upon considering the materials in both the coating and the half-space layers to be the same, one sets $\mho = \frac{c_1}{c_2} = 1$, and eventually obtains from Eq. (48) that both velocities trend to unity as follows

$$\text{Phase velocity} = \text{Grough velocity} \approx 1. \tag{49}$$

What is more, Figures 6 and 7 examined the acquired velocity curves in Eq. 47, assessing the significance of varying the Winkler-Fuss foundation parameter X, and the shear speed ratio $\mho$, respectively. In particular, upon varying the Winkler-Fuss foundation parameter (indeed, a soft foundation with $X = 0.01, X = 0.02, X = 0.03$), one notes from Figure 6 that an increase in the foundation parameter increases the group velocity, while decreasing the phase velocity. In addition, Figure 7 captures the evolution of the related velocities with the variation in shear speed ratio. In fact, when considering the shear speed ratio $\mho = 1$, that is, when both the coating and the half-space are made of the same materials, both velocities are noted to assume the least values. Indeed, one observes that an increase in the shear speed ratio decreases both velocity profiles. Moreover, one observes from both Figures 6 and 7 that both velocities met at unity upon considering no Winkler-Fuss foundation.

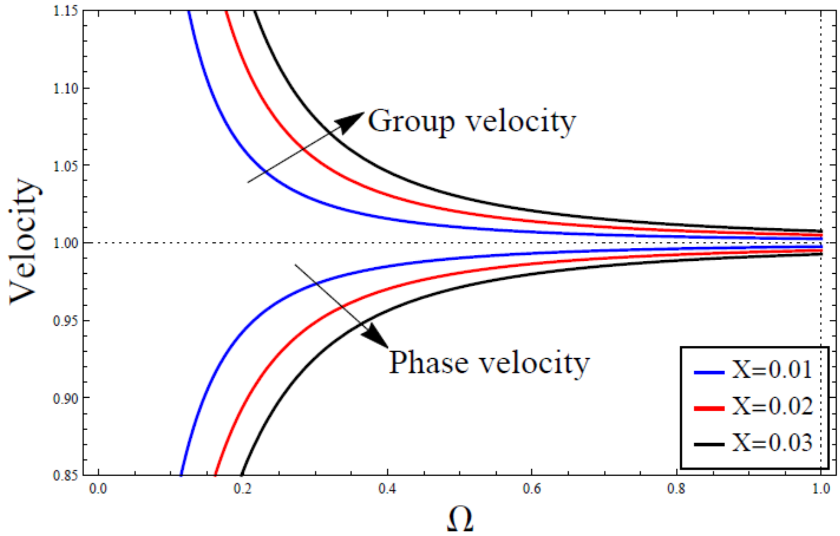

Figure 6: Significance of Winkler-Fuss foundation parameter X on the variation of velocities Eq. (47) when $\mho = 1$.

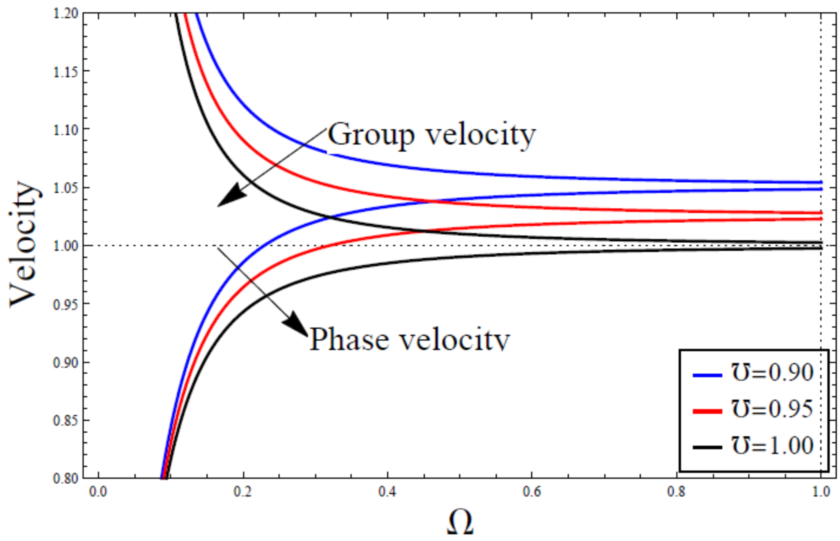

Figure 7: Significance of shear speed ratio Ʊ on the variation of velocities Eq. (47) when $X = 0.01$.

8 Conclusion

The present study examined the propagation of surface waves on a coated cylindrical half-space amidst the influence of generalized imperfect interfacial conditions and the Winkler-Fuss elastic foundation, which served as a mechanical load on the coating medium. An analytical method of solution, together with an approximation method, has been sought to derive the consequential dispersion relation aside from the acquisition of the overall vibrational displacements in the respective layers. In particular, an approximate equation for anti-plane motion has been obtained using the asymptotic approximation method, assuming the interfacial imperfection is absent. Moreover, some realistic contrast setups showed, through the numerical study, that an increase in the sliding contact parameter Ψ increases the dispersion of waves in the coated medium, while noting the increase of the Winkler-Fuss elastic foundation parameter X to decrease the dispersion of waves in the medium under the action of a stiff elastic foundation. Further, maximum rise has been noted to be associated with the aluminum ratio zinc material (the least) among the competing ratios. In addition, the derived approximate result has been noted to agree with the corresponding analytical result. Additionally, the derived approximate expressions for the phase and group velocities have been examined, which showed in-depth salient characteristics of waves in the medium, which could not easily be deduced from the analytical analysis - that the significance of mechanical loading and the shear speed ratio on the propagating shear waves in the coated medium is pronounced. In the end, this study applies to the burning areas of material and geophysical sciences, where methods and in-depth understanding are needed to devise smart materials, and, on the other hand, to the exploration of buried minerals, where multiple layers with dissimilar properties are uncovered. What is more, future undertakings could be directed towards multi-layering, in addition to the incorporation of several forces.

Acknowledgements

The authors would like to acknowledge Deanship of Graduate Studies and Scientific Research, Taif University for funding this work.

Funding

This work was funded by the Deanship of Graduate Studies and Scientific Research, Taif University.

Conflict of interest

The author declares that she has no conflicts of interest to this work.

Nomenclature

Dimensional quantities

c_p Shear speed, $p = 1, 2$
h thickness of the coating
k Wavenumber
t time
L wave length
χ Stiffness of Winkler-Fuss foundation
u_p, v, Displacement, $p = 1, 2$
μ_p Lame's constant, $p = 1, 2$
ρ_p Density, $p = 1, 2$
ω Frequency
ψ Imperfect contact parameter
τ_{23}^p Shear stress, $p = 1, 2$

Dimensionless quantities

R, η scaled thickness
u_p^*, v^* Displacement, $p = 1, 2$
τ time
K Frequency

X, χ^* Stiffness of Winkler-Fuss foundation
Ψ Imperfect contact parameter
Ω Wavenumber
μ Lame's constant ratio
ρ Density constant ratio
$\mho$ Shear speed ratio
ε length ratio
τ_{23}^* Shear stress

References

[1] Shatskyi, I., Makoviichuk, M., Ropyak, L., Velychkovych, A. Analytical model of deformation of a functionally graded ceramic coating under local load. Ceramics, 6, (2023) 1879–1893.

[2] Mubaraki, A.M., Helmi, M.M., Nuruddeen, R.I. Surface wave propagation in a rotating doubly coated. Symmetry, 14, (2022) 1000.

[3] Dai, H.H., Kaplunov, J., Prikazchikov, D.A. A long-wave model for the surface elastic wave in a coated half-space. Proc. Royal Soc. A: Math. Phys. Eng. Sci. 466, (2010) 3097-3116.

[4] Helmi, M.H., Althobaiti, S., Mubaraki, A.M., Rogerson, G.A. Asymptotic formulations of anti-plane problems in pre-stressed compressible elastic laminates. Open Phys. 21, (2023) 20220265.

[5] Mubaraki, A.M., Almalki, F.M. Surface waves on a coated homogeneous half-space under the effects of external forces. Symmetry, 14, (2022) 2241.

[6] Mubaraki, A.M., Helmi, M.M., Nuruddeen, R.I., Areshic, M. Propagation of Rayleigh-type waves on an elastic half-space covered by a thin multi-layered coating. Mech. Solids, 59 (2024), 2906–2920.

[7] Ebrahiminejad, A., Mardanshahi, A., Kazemirad, S. Nondestructive evaluation of coated structures using Lamb wave propagation. Appl. Acoust. 185, (2022) 108378.

[8] Selim, M.M. Effect of thermal stress and magnetic field on propagation of transverse wave in an anisotropic incompressible dissipative initially stressed plate. Appl. Math. Inf. Sci. 11, (2017) 195-200.

[9] Ebrahimi, F., Barati, M.R., Dabbagh, A. Wave propagation in embedded inhomogeneous nanoscale plates incorporating thermal effects. Waves Random Compl. Media, 28 (2018) 215-235.

[10] Erbas, B., Kaplunov, J., Nobili, A., et al. Dispersion of elastic waves in a layer interacting with a Winkler foundation. J. Acoust. Soc Am. 144(5), (2018) 2918-2925.

[11] Ebrahimi, F., A. Seyfi. A wave propagation study for porous metal foam beams resting on an elastic foundation. Waves Random Compl. Media, 31, (2021) 1-15.

[12] Shaat, M., Gao, X.-L., Battentier, A., Massue, N. New analytical model for multi-layred composite plate with imperfect interfaces under thermomechanical loading. Acta Mach. 235, (2024) 7083–7120.

[13] Nuruddeen, R.I., Mubaraki, A.M. Propagation of damped SH waves on nonhomogeneous elastic composites involving viscoelasticity, generalized interface, rotation and mechanical loading. Ain Shams Eng. J. 15 (2024), 103053.

[14] Hetenyi, M. Beams on Elastic Foundation. 4th printing: Ann Arbor, Michigan, The University of Michigan Press, (1955).

[15] Wang, Y.H., Tham, L.G., Cheung, Y.K. Beams and plates on elastic foundations: a review. Prog. Struct. Engng Mater. 7, (2005) 174-182.

[16] Younesian, D., Hosseinkhani, A., Askari, H., Esmailzadeh, E. Elastic and viscoelastic foundations: a review on linear and nonlinear vibration modeling and applications. Nonlinear Dyn. 97, (2019) 853-895.

[17] Ghazwani, M.H., Alnujaie, A., Vinh, P.V. A general viscoelastic foundation model for vibration analysis of functionally graded sandwich plate with auxetic core. Defence Techn. (2025).

[18] Kumari, C.; Kundu, S.; Kumari, A.; Gupta, S. Analysis of dispersion and damping characteristics of Love wave propagation in orthotropic visco-elastic FGM layer with corrugated boundaries. Int. J. Geomech. 20, (2020) 04019172.

[19] Saha, S., Singh, A.K., Chattopadhyay, A. On propagation behavior of SH-wave and Rayleigh-type wave in an initially stressed exponentially graded fiber-reinforced viscoelastic layered structure. Waves Random Compl. Media, 31, (2021) 486–514.

[20] Kumari, P., Sharma, V.K. Propagation of torsional waves in a viscoelastic layer over an inhomogeneous half-space. Acta Mech. 225, (2014) 1673–1684.

[21] Abd-Alla, A.M., Abo-Dahab, S.M., Khan, A. Rotational effects on magneto-thermoelastic Stoneley, Love, and Rayleigh waves in fibre-reinforced anisotropic general viscoelastic media of higher order. Comput. Mater. Cont. 53, (2017) 49–72.

[22] Elmoghazy, Y.H., Safaei, B., Asmael, M., Sahmani, S., Zeeshan, Q., Qin, Z. Computational modelling and analysis of effect of viscoelastic materials on damping and vibrational behaviors of composite structures—An extensive review. Arch. Computa. Meth. Eng. 31, (2024) 2611–2662.

[23] Bullen, K.E. The problem of the density variation. Bul. Seismol. Soc. Amer. 30(3) (1940) 235-250.

[24] Althobaiti, S., Mubaraki, A.M., Nuruddeen, R.I. Dispersion of flexural waves on an initially prestressed thin plate resting on nonlinear elastic foundations. Acta Mech. (2025).

[25] Marin, M.I., Agarwal, R.P. Abbas, I.A. Effect of intrinsic rotations, microstructural expansion and contractions in initial boundary value problem of thermoelastic bodies. Bound. Val. Probl. 129, (2014).

[26] Abouelregal, A. E., Marin, M., and Ãchsner, A. (2023). The influence of a non-local Moore-Gibson-Thompson heat transfer model on an underlying thermoelastic material under the model of memory-dependent derivatives. Continuum Mechanics and Thermodynamics, 35(2), 545-562..

[27] Zeeshan, A., Khan, M.I., Ellahi, R., Marin, M. Computational intelligence approach for optimising MHD Casson ternary hybrid nanofluid over the shrinking sheet with the effects of radiation. Appl. Sci., 13(17), (2023) 9510.

[28] Althobaiti, S., Nuruddeen, R.I., Mubaraki, A.M. Elastodynamics of a damped coated half-space under the influence of rotation, Pasternak foundation and generalized contact conditions. J. Vibr. Eng. Tech. 13(336), (2025).

[29] Horgan, C.O. Anti-plane shear deformations in linear and nonlinear solid mechanics. SIAM Rev. 37, (1995) 53-81.

[30] Madan, D.K., Kumar, N., Muwal, R. Dispersion of Love wave in a viscoelastic sandy layer overlying anisotropic half-space with parabolic interface. Jnanabha. 54(1), (2024) 244-253.

[31] Acharya, D.P., Roy, I. Effect of surface stress and irregularity of the interface on the propagation of SH-waves in the magneto-elastic crustal layer based on solid semi space. Sadhama, 34, (2009) 309-330.

[32] Kumari, P., Sharma, V.K. Propagation of torsional waves in a viscoelastic layer over an inhomogenous half space. Acta. Mech. 225, (2014) 1673-1684.

[33] Nuruddeen, R.I., Nawaz, R., Zia, Z.Q.M. Effects of thermal stress, magnetic field and rotation on the dispersion of elastic waves in an inhomogeneous five-layered plate with alternating components, Sci Progr. 103(3), (2020) 1-22.

[34] Mubaraki, A.M. Asymptotic consideration for Rayleigh waves on a coated orthorhombic elastic half-space reinforced by the elastic Winkler foundation. Math. Comp. Appl. 28(109), (2023).

[35] Mubariki, A., Prikazchikov, D. On Rayleigh wave field induced by surface stresses under the effect of gravity. Math. Mech. Sol. (2020) 1–12.